AIAA JOURNAL
Vol. 31, No. 8, August 1993

Organized Structure in a Compressible Turbulent Shear Layer

Y. R. Shau,* D. S. Dolling,† and K. Y. Choi‡
University of Texas at Austin, Austin, Texas 78712

An experimental study has been made of the large-scale structures in a two-dimensional, high Reynolds number, turbulent free shear layer bounded by Mach 5 and 3 airstreams. The convective Mach number was about 0.28. Mean pitot pressure surveys were made to determine the shear layer growth rate, the two-dimensionality, and the external flowfield. Two-point fluctuating pitot pressure measurements were made to investigate the large-scale structure at several stations from 600 to 2450 initial momentum thicknesses θ_0 downstream of the shear layer origin. Power spectra show increasing organization with distance downstream, and at 2450 θ_0, the large-scale structures are responsible for a strong concentration of energy between 16 and 25 kHz. In nondimensional terms, the power spectra are centered at a Strouhal number of about 0.35. The large-scale structures are inclined at about 42–48 deg to the flow direction, which agrees well with schlieren photographs. Cross correlations of spanwise pitot pressure signals show that the spanwise extent of the large-scale structure is only about 1.0–1.5 shear layer thicknesses. Results from a preliminary study using fixed-spacing dual normal hot wires agree very well with results from fluctuating pitot pressures.

Nomenclature

a = speed of sound
f = frequency
f' = focal length of the optical lens
$G(f)$ = power spectral density
M = Mach number
M_c = convective Mach number
U_c = convection velocity
u = streamwise mean velocity
x = streamwise location from the trailing edge of the model
y = vertical location from the upper surface of the model
y^* = vertical location referenced to the Mach 3 edge of the shear layer
β = inclination angle of the large-scale structure to the horizontal axis
Δ_y = vertical spacing between two probes
Δ_z = spanwise spacing between two probes
δ = shear layer thickness
δ_{pt} = shear layer thickness based on 5–95% or 95–95% pitot pressure profile
δ_{rms} = shear layer thickness based on fluctuating pitot pressure rms
δ_{vis} = shear layer thickness based on flow visualization
θ_0 = momentum thickness at the shear layer origin
λ = velocity ratio, $(u_1 - u_2)/(u_1 + u_2)$
σ = rms of fluctuations (or standard deviation)
τ = cross-correlation time delay
τ_p = time delay at the maximum cross correlation

Subscripts

1 = higher speed mean flow (Mach 5)
2 = lower speed mean flow (Mach 3)

Presented as Paper 92-0180 at the AIAA 30th Aerospace Sciences Meeting, Reno, NV, Jan. 6–9, 1992; received Jan. 22, 1992; revision received Oct. 7, 1992; accepted for publication Oct. 12, 1992.

*Postdoctoral Fellow, Department of Aerospace Engineering and Engineering Mechanics; currently Associate Professor, Institute of Applied Mechanics, National Taiwan University, Taipei 106, Taiwan. Member AIAA.

†Professor, Department of Aerospace Engineering and Engineering Mechanics.

‡Graduate Research Assistant, Department of Aerospace Engineering and Engineering Mechanics. Student Member AIAA.

Introduction

DEVELOPMENT of airbreathing hypersonic vehicles has sparked widespread interest in supersonic combustion, since a possible propulsion option is the supersonic combustion ramjet engine (scramjet). In such an engine, fuel-rich flow is mixed with a supersonic airstream. Combustion efficiency is of great concern since the growth and entrainment rates of compressible shear layers are known to be much smaller than those of incompressible flows at the same velocity and density ratios. To improve the growth rate or mixing of a compressible shear layer, an understanding of the shear layer structure and the mechanism that controls the mixing is clearly important.

Theoretical and experimental studies[1–4] have shown that shear layer growth rate correlates reasonably well with the convective Mach number M_c, which is the Mach number of the freestream relative to the moving reference frame of the large-scale structures in the flow. Brown and Roshko[5] first observed that the incompressible mixing layer was dominated by large-scale organized structures that grew in size and spacing and convected downstream at nearly constant speed. Several flow visualization investigations have shown that large-scale structures also exist in supersonic shear layers. Clemens,[6] Clemens and Mungal,[7] and Clemens et al.[8,9] used Mie scattering from condensed alcohol droplets and planar laser-induced fluorescence of nitric oxide to examine the structure of a planar mixing layer at $M_c = 0.28$, 0.62, and 0.79. Results show the characteristic two-dimensional Brown and Roshko structure at low M_c but increasing three-dimensionality with increasing M_c. The change in structure was due to compressibility, not Reynolds number. Elliott et al.[10] and Elliott and Samimy[11] also noted substantial three-dimensionality in a planar shear layer with $M_c = 0.51$. Time-series analyses of fluctuating pressures were used to obtain estimates of streamwise structure scale and spacing. Values of 1.3 and 4.5 times the vorticity thickness, respectively, were obtained in the fully developed region. Messersmith and Dutton[12] used the same techniques, at relative Mach numbers Mr ($\equiv 2\Delta u/a_1 + a_2$) of 0.63, 0.98, and 1.49 to examine the large-scale structure and the probability density functions of passive scalar transport to assess mixed fluid probability. Note that the relative Mach number is twice the convective Mach number for gases of equal specific heat ratios. As Mr increased, the dimensionless structure size and eccentricity in the transverse plane (i.e., side view) increased, whereas structure angles relative to the freestream direction decreased. Oblique images (at 60 deg to the flow direction) showed significant three-dimensionality with increasing compressibility, consistent with the findings of Refs. 7 and 10. These experimental observations are consistent with numerical studies,

employing both linear stability[4] and direct simulations of the compressible Navier-Stokes equations.[13] At low M_c (<0.4), numerical work shows that the two-dimensional Kelvin-Helmboltz instability plays a dominant role, whereas at higher M_c (>0.6), three-dimensional modes are dominant.

The focus of the current study was to examine the large-scale structures in a high Reynolds number, supersonic, turbulent shear layer at a relatively low convective Mach number ($M_c \approx 0.3$). The work is part of a program to investigate the effects of initial conditions on the growth rate and large-scale structures. In an earlier study,[14] the developing region (i.e., $x \leq 12.7$ cm) of the shear layer was investigated. At $x = 12.7$ cm, it was found that the large-scale structures were not yet highly organized. Further, the initial region of the shear layer had a wakelike character, such that the large-scale structure shape and orientation were affected, and it appeared that two substructures existed within each large-scale structure. To examine the evolution further downstream, a longer wind-tunnel test section was built, which allows measurements to be made up to about 2500 initial momentum thicknesses downstream of the shear layer origin. It was anticipated that a more highly organized structure would exist at that station.

In the present study, standard pitot pressure probe and pitot rake surveys were made to determine the growth rate and two-dimensionality of the shear layer. Two-point fluctuating pitot pressure measurements were also made to detect the large-scale structure of the shear layer up to 52 cm (2450 θ_0) downstream of the shear layer origin. From these measurements, cross correlations of the signals were calculated to determine the orientation and extent of the large-scale structures. Both streamwise and spanwise results are presented. Schlieren photography was also used to visualize the turbulent structures in two regions bounded by $x = 18-25$ and $x = 42-52$ cm. Since the method provides a spanwise-integrated view of the flow features, it is not suitable if significant three-dimensionality occurs. In this case, for a shear layer with low convective Mach number, it was expected that the large-scale structures would be quasi-two-dimensional, and it was hoped that schlieren would be a valuable tool. Finally, fixed-spacing dual normal hot-wire measurements were used to study the large-scale structures at $x = 48$ cm. Comparisons of the results from all three methods are presented in this paper.

Experimental Program

Wind Tunnel and Model

The experiments were conducted in the Mach 5 blowdown tunnel of the University of Texas Wind-Tunnel Laboratories at the Balcones Research Center. The tunnel has a cross section of 17.75×15.24 cm and has adjustable stagnation pressure and temperature. The model that generates the shear layer is a flat plate with an internal converging-diverging Mach 3 nozzle and has been described in detail by Shau.[15] A schematic of the setup is shown in Fig. 1. The plate is 35.6 cm long, 15.24 cm wide, and 1.91 cm thick with an 8-deg biwedge leading edge. It is installed at zero angle of attack on the test section centerline. The internal Mach 3 nozzle contour was designed using a method-of-characteristics code with a correction for boundary-layer displacement thickness effect, and the nozzle exit is at the trailing edge of the plate. The ceiling and floor of the test section are slotted to allow probes to be positioned with effectively infinite resolution.

Air Supply

To have both streams at the same stagnation temperature, the air supplies for the Mach 5 tunnel and Mach 3 nozzle share the same source. Thus, both streams are air. Atmospheric air was compressed using a Worthington four-stage compressor, passed through filters, and then stored in a 4 m^3 tank at 17.2 MPa (2500 psig). A control valve monitored by a microprocessor regulates the flow into the Mach 5 tunnel. Before entering the tunnel, the air passes through a series of electric heaters to raise its stagnation temperature. A fraction of the heated air in the Mach 5 stagnation chamber is bypassed to a second control valve that is also monitored by a microprocessor and then enters the Mach 3 nozzle. The stagnation pressures for both streams are set to match the static pressures at the shear layer origin. To avoid temperature drops, the pipes that direct the air to the Mach 3 nozzle are wrapped with heating tape and covered with thermal insulation. Before the test, the pipes were preheated to the stagnation temperature of the flow. Thus, during the experiment, heat transfer from the airflow to the pipes is minimized. The air enters the model through slots on both sides. A double screen assembly is installed in the plate to prevent large vortex structures generated by the turning vane from exiting the Mach 3 nozzle. The maximum run time is about 60 s.

Instrumentation/Data Acquisition

The mean shear layer profile development on tunnel centerline was investigated using a standard pitot probe with a rectangular opening about 0.2 mm high and 1.3 mm wide. For a fast response, a Kulite pressure transducer (Model XCQ-062-50A) was installed in the probe shaft. To assess the two-dimensionality of the shear layer, a seven-tip pitot rake was used. Each of the rake tips had the same dimensions as the single tip probe. The tip center-to-center distance was 1.27 cm, for an overall span of 7.6 cm. Again, for a fast response, each tip was connected to a separate pressure transducer (Kulite Model OEM-CTQH-187) installed in the rake. The vertical position of the probe tip was measured using a Schaevitz dc-operated linear variable differential transformer (LVDT) model 6000. It has a range of ±7.6 cm with an output at full displacement of ±10 V. A dial gauge with an accuracy of ±0.025 mm was used to calibrate the LVDT and to measure the spacing between probe tips.

Fluctuating pitot pressures were measured using probes in which high-frequency response miniature Kulite transducers (Model XCQ-062-50A) were installed in the probe tip with the transducer face normal to the stream. The transducer had a range of 0–345 kPa and a nominal full-scale output of 75 mV. The outer diameter of the transducer is 1.6 mm with a pressure sensing area of 0.77 mm in diameter. To protect the transducer from any high momentum dust particles in the airstream, a perforated screen is installed above the diaphragm. The frequency response of these impact pressure probes is about 60 kHz. Output from the Kulite pressure transducers was amplified and then lowpass filtered using analog filters, with the cut-off frequency set to 63 kHz. The filtered signals were then digitized by a LeCroy-6810 waveform recorder employing a 12-bit A/D converter. Typically, the signal-to-noise ratio was about 100.

For the fluctuating pitot pressure measurements, data were sampled at 500 kHz per channel, and 128 records (1024 data points per record) were taken at 16 different y positions in the shear layer at a given streamwise station. For the variable-spacing, two-probe measurements, one probe was held at a fixed position and the other probe was moved away from it in fixed increments. For the fixed-spacing, two-probe measurements, the probe tips had center-to-center spacing of 4.16 mm and were moved as a unit through the flowfield.

The schlieren system consists of an EG&G Microflash System 549 with spark point light source (which has nominal pulse duration of about 0.5 μs), two optical lenses (one is 10.16 cm in diameter, $f = 86.36$ cm, and the other is 11.43 cm in diameter; $f = 101.6$ cm), a razor blade knife edge, and a Polaroid 4×5 camera. The viewing window is 10.16 cm in diameter.

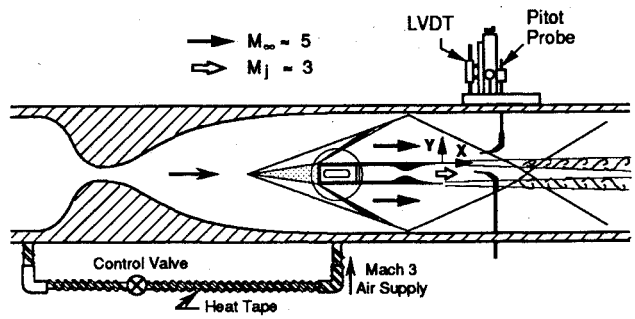

Fig. 1 Experimental setup.

Two parallel normal hot wires with spacing 2.6 mm were also used to investigate the large-scale structure and determine the corresponding structure angles. The hot wires were made of platinum-plated tungsten wires 5 μm in diameter and about 0.8–1.0 mm in length. The dual normal-wire probe was connected to two DANTEC constant temperature anemometers with DISA-55M10 standard bridges (bridge ratio 20:1). The frequency response of the hot wires, as determined from a sine wave test, was about 125 kHz. The signal output from the anemometers was processed by low-pass filters set at 125 kHz to prevent aliasing and sampled at 500 kHz per channel.

Analysis Techniques

Standard time-series analysis techniques have been used extensively to examine the data. Power spectral density coefficients $G(f)$ in psia^2/Hz were calculated inversely by using the standard fast Fourier transform (FFT) method that analyzes one record at a time and outputs 512 spectral coefficients. Since the sampling rate is 500 kHz, this results in a frequency resolution of 488 Hz. Cross correlations were calculated from the inverse FFT transform of the cross-spectral density function. For details of these techniques, the reader is referred to Bendat and Piersol.[16] From the time delay τ_p at the maximum cross-correlation coefficient, the large-scale structure average inclination angle β can be estimated

$$\beta = \tan^{-1}(\Delta y / U_c \tau_p) \quad (1)$$

Theoretically, the convection velocity can be calculated from[3,4]

$$U_c = (u_1 a_2 + u_2 a_1)/(a_1 + a_2) \quad (2)$$

It should be noted that recent experiments (Refs. 17–20) have indicated that the large structures do not convect downstream at the velocity given by Eq. (1). A discussion of these results and others is given by Dimotakis,[21] who presents a method to estimate U_c in low Mach number shear layers. In the current experiment, the two streams differ in velocity by approximately 100 m/s ($U_1 = 763$ m/s, $U_2 = 675$ m/s). For a structure angle β of about 45 deg, an uncertainty in U_c of ±20 m/s corresponds to an uncertainty in β of only ±0.8 deg. The time delay τ_p from the cross correlation is more critical. Since the resolution is limited by the sampling rate (i.e., 2 μs for a sampling frequency of 500 kHz), the time delay τ_p at maximum correlation is extracted from a five-point, third-order, polynomial curve-fit of the original cross-correlation data.

Table 1 Mach 5 boundary-layer properties

Mach number, M_∞	4.90
Boundary-layer thickness, mm, $\delta_{0.99}$	4.7
Displacement thickness, mm, δ^*	2.5
Momentum thickness, mm, θ	0.21
Shape factor, H	11.6
Reynolds number, Re_θ	9600
Wake parameter, II	0.84
Skin friction coefficient, C_f	0.00091
Wall shear-stress, N/m^2, τ_w	66
Shear layer convective Mach number at origin, M_c	0.28

Discussion of Results

Mean Flowfield and Shear Layer Growth Rate

The Mach 5 boundary layer on the plate undergoes natural transition and becomes fully turbulent upstream of the shear layer origin. The boundary-layer properties at the shear layer origin, using standard nomenclature, are listed in Table 1.

Although the boundary layer on the Mach 3 side was not measured due to its size ($\delta < 0.6$ mm), it is believed to be laminar based on the Reynolds number. Figure 2 shows the pitot pressure evolution of the shear layer on the centerline of the tunnel (i.e., $z = 0$). Each profile's streamwise position is indicated by a vertical arrow on the top and bottom along the x axis. The pitot pressure (in psia) of the Mach 3 flow at midcore for each profile is also labeled next to the profile. The wake deficit (which is marked with a "W") is evident in the pitot pressure profiles in the developing region (i.e., $x = 0.4 - 33$ cm) and disappears further downstream (i.e., $x > 38$ cm). Because of the finite thickness of the nozzle trailing edge, compression and expansion waves originating from the nozzle lip cannot be completely eliminated. The effects can be seen in the pitot profiles. In addition, the two shock waves originating from the plate leading edge (Fig. 1) are reflected from the tunnel ceiling and floor and cross the shear layer about 29 cm downstream of the origin. Although there is compression and turning of the shear layer due to these shock waves, it is obvious that the potential core of the Mach 3 jet persists far downstream in the flowfield. Even at $x = 50$ cm, it is still about 0.6 cm thick. Cross correlations and coherence function results show no interaction between upper and lower shear layers.

Rake surveys of the boundary layer just upstream of the shear layer origin and in the shear layer up to $x = 23$ cm downstream showed that the mean flow is essentially two dimensional. Further downstream, the spanwise variation in the shear layer thickness increases. The crossing shocks introduce streamwise and spanwise pressure gradients that result in an increase in three-dimensionality. However, pitot rake surveys at $x = 38$, 43, and 48 cm (i.e., downstream of the shock impingement) show that the shear layer is still two dimensional over the central 5.2 cm. Flow conditions were very repeatable from test to test. The mean flow conditions for the entire flowfield are shown in Fig. 3, and the mean properties (i.e., Mach number, total pressure, and velocity) in each region are tabulated below the figure.

The shear layer thickness as a function of streamwise position is shown in Fig. 4. The thickness has been deduced three ways: 1) from mean pitot pressure profiles (δ_{pt}), 2) from the fluctuating pitot pressure rms distributions and probability density functions (δ_{rms}), 3) from schlieren photographs (δ_{vis}). The pitot pressure thickness

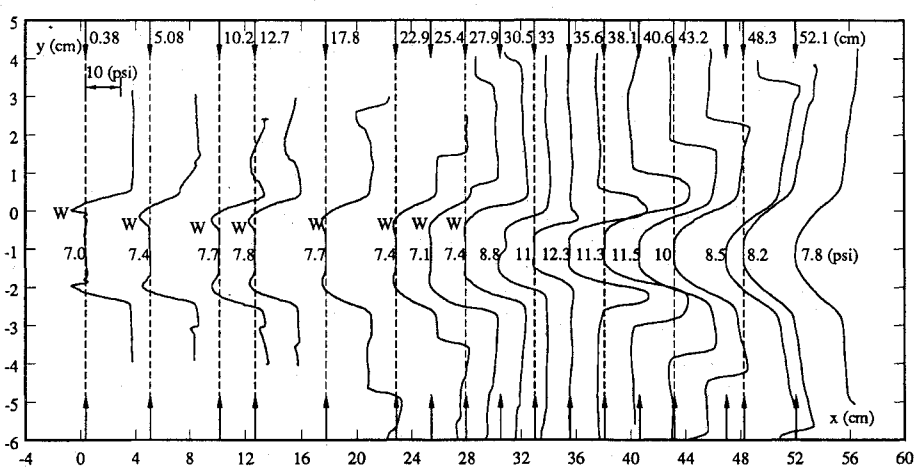

Fig. 2 Mean pitot pressure evolution.

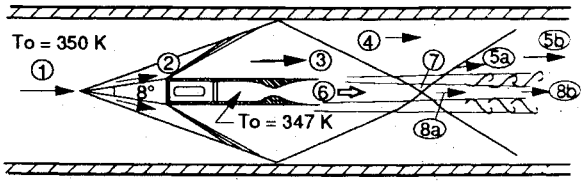

Region	Mach Number	Stagnation Pressure (N / m^2)	Velocity (m/sec)
1	4.95	2.096 x 10^6	765
2	4.60	2.068 x 10^6	753
3	4.90	2.068 x 10^6	763
4	4.75	2.023 x 10^6	760
5a	4.20	1.986 x 10^6	740
5b	4.70	1.986 x 10^6	758
6	3.05	1.551 x 10^5	675
7	2.75	1.543 x 10^5	650
8a	2.40	1.536 x 10^5	610
8b	2.95	1.536 x 10^5	665

Fig. 3 Mean flowfield details.

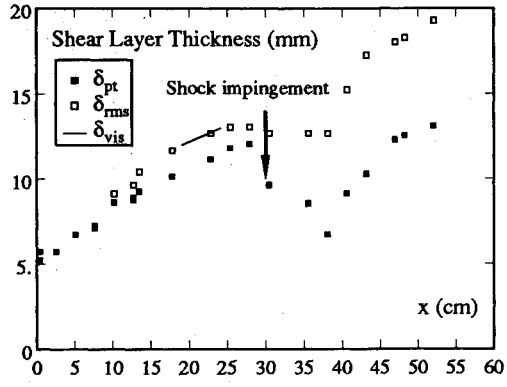

Fig. 4 Shear layer thickness as a function of streamwise position.

δ_{pt} is based on 95–95% of the pitot deficits when the profile exhibits wake behavior and is based on 5–95% of the pitot deficit for profiles without a wake.[3] Because of the intermittency of the large-scale structures, the edges of the shear layer can also be determined from the probability density distribution of the fluctuating pitot pressure signals. Also, the rms of the fluctuating pitot pressure decreases to a constant value when the probe enters the Mach 5 or 3 mean flow. Thus, the rms thickness δ_{rms} can be determined from the behavior of rms and probability density functions. Visual thickness δ_{vis} is measured by drawing a straight line tangent to the edge of the shear layer from schlieren photographs. For relatively small growth rates, this method has a high uncertainty.

Since the shear layer exhibits a wakelike behavior only in the developing region, the method used to define the pitot thickness is not the same as that used at downstream stations. This change in definition and the compression due to the shock impingement at $x = 29$ cm are the cause of the large decrease in the pitot thickness δ_{pt} when the wakelike behavior disappears (i.e., $x \approx 30$ cm). This is unavoidable since a consistent definition cannot be employed. Nevertheless, with or without a wake, both definitions give a linear growth of low magnitude, as expected. Since the rms thickness reveals the vertical extent of the large-scale structures, the agreement between δ_{rms} and δ_{vis} is good, whereas $\delta_{rms} > \delta_{pt}$. Although the physical length scales are different, the pitot thickness growth rate is essentially the same as the value based on the rms thickness. At $x \approx 21.6$ cm, the shear layer growth rate based on all three definitions is essentially the same. The growth rate is about 90% of its incompressible value at the same velocity and density ratio. Effects of the shock impingement on the shear layer growth rate are evident in Fig. 4. Just downstream of the shock impingement the growth rate increases substantially but rapidly returns to its undisturbed value further downstream. From the development of the rms thickness, it is also clear that the shear layer thickness is affected and remains essentially constant through the region of compression by the shock wave. Once the shock wave leaves the shear layer, the thickness increases at a higher rate and returns to its original value (i.e., the value extrapolated from the growth rate before the shock impingement).

Large-Scale Structures

Investigation of the large-scale structures was performed at several streamwise positions at which both single-probe and two-probe fluctuating pitot pressure measurements were made. Power spectra of the fluctuating pitot pressure at two stations ($x = 22.9$ and 47 cm or 1090 and 2240 θ_0, respectively) are shown in Figs. 5a and 5b. The frequency has been nondimensionalized to form a Strouhal number ($St = f\,\delta_{pt}/U_c$). The upper seven curves of each figure are y offset 0.5 units with respect to the curve below it. The corresponding positions of the probe are indicated in the mean pitot profile above each figure. In Fig. 5a, it is evident from the pitot pressure profile that the wake behavior still exists in the shear layer. When the probe is located in the Mach 3 mean flow, the signal has a broadband, flat spectrum and a very low rms. The major contribution to the overall rms comes from components in the higher frequency range (i.e., $f > 35$ kHz). As the probe enters the wake deficit region of the shear layer on the lower speed side (i.e., stations 2 and 3), the energy at higher frequency increases and the rms increases slightly as would be expected. When the probe is moved above the minimum velocity point (stations 4, 5, 6, and 7), the spectra are essentially the same. At $x = 1090\ \theta_0$ (Fig. 5a), the energy content is relatively broadband in the range $0.20 \le St \le 0.55$ (13–36 kHz) with the peak centered at $St \approx 0.37$. Since the frequency response of the probe is on the order of 60 kHz, these data are well within its dynamic range and can be considered reliable. Once the probe enters the Mach 5 freestream (station 8), the power spectrum of the signal is again similar to that observed at station 1. It is evident that there is a clear shift in frequency from station 3 to 4 across the minimum velocity position. Other evidence from time-series analysis (i.e., probability density function, coherence function, time delay) suggests that two vortical structures coexist within the large-scale structure due to the wakelike behavior. This was described in an earlier study.[22] In Fig. 5b, at $x = 2240\ \theta_0$ where

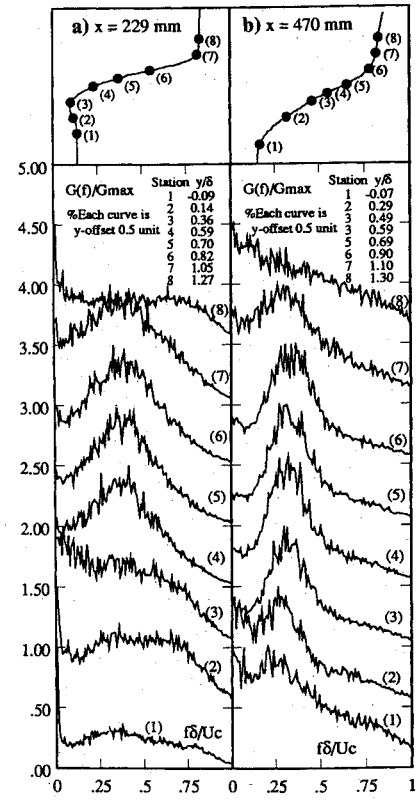

Fig. 5 Normalized power spectra across shear layer: a) $x = 22.9$ cm and b) $x = 47$ cm.

the wake behavior has disappeared, the passage of the large-scale structures generates a strong peak in the frequency range of about $0.25 \le St \le 0.45$ (16–32 kHz) now centered at $St \approx 0.33$. Thus, the large-scale structures have become more organized at this station ($x = 2450\ \theta_0$) and the wake behavior has disappeared.

The progressive organization with distance downstream is even more evident from examination of power spectra measured at the same relative position (i.e., the local maximum in rms) in the shear layer but at many streamwise stations (Fig. 6). All curves are again y offset 0.5 units with respect to the curve below. The sharpening of energy spectra at the preferred frequency of the large-scale structures is obvious. The peak of the power spectra is centered at about 30 kHz at $x = 850\ \theta_0$ (17.8 cm) and is reduced to about 20 kHz at $x = 2480\ \theta_0$ (52 cm). The results obtained from hot wires at $x = 48.3$ cm agree very well with the fluctuating pitot pressure measurements, confirming that the fast-response pitot probe is quite capable of resolving the dynamics of this type of flowfield.

Comparison of the normalized power spectrum measured at $x/\theta_0 = 2240$ with those measured in incompressible flow by Browand and Ho[23] is shown in Fig. 7. Browand and Ho investigated the incompressible mixing between two airstreams with a velocity ratio, $\lambda = 0.65$, in which the large-scale structure was judged organized and quasi-two-dimensional. The power spectra from hot-wire data in the fully developed region (i.e., $300 < x/\theta_0 < 1210$) are broadband and have a similar bandwidth as the current case. The normalized frequency is centered at a Strouhal number of about 0.2 for the incompressible shear layer (based on the vorticity thickness). For the compressible case, the peak of the spectrum is centered at about 0.35 (which is also evident in Figs. 5 and 6). The shear layer thickness δ used for the current case is the pitot thickness which is about 20–25% larger than the vorticity thickness. The similarity in spectra suggests the existence of organized structures in the compressible case. However, the compressible case is not quasi-two-dimensional as explained later.

Figure 8 shows cross correlations of two-point variable-spacing pitot pressure measurements at $x = 38.1$ cm (1815 θ_0). The positions of the probes are indicated in the mean pitot profile. One of the probes (channel 2) was fixed at the Mach 3 edge of the shear layer, whereas the upper probe (channel 1) was moved from station a to f. Because of the existence of large-scale structures, the two signals are highly correlated. As the probe spacing increases,

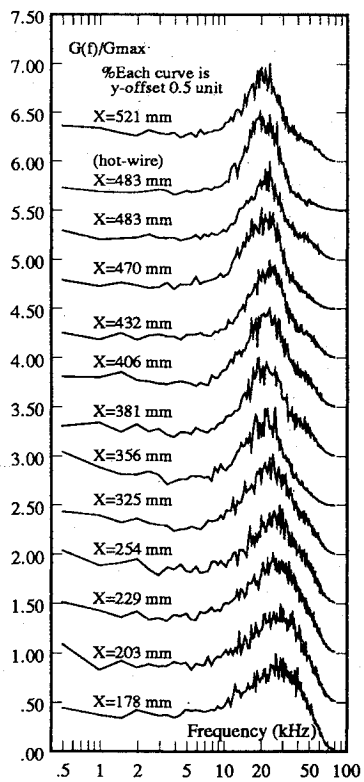

Fig. 6 Normalized power spectra evolution.

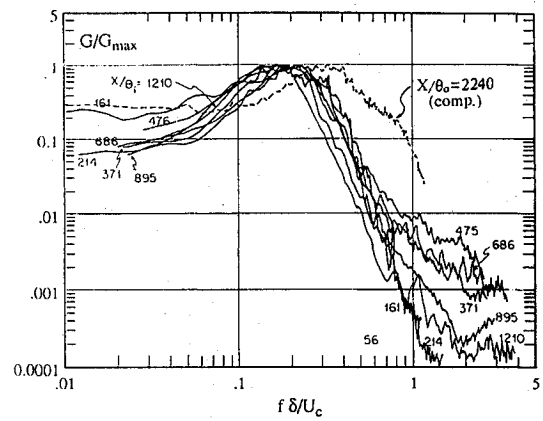

Fig. 7 Comparison of normalized power spectrum at $x = 2240\ \theta_0$ with incompressible results of Ref. 23.

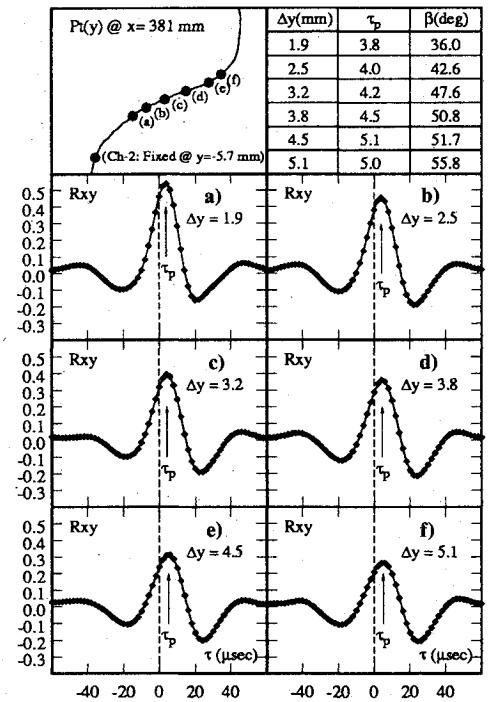

Fig. 8 Cross correlations at $x = 38.1$ cm (variable probe spacing with fixed probe at $y = -5.7$ mm).

the cross-correlation coefficient magnitude decreases as expected. Based on the time delay at maximum cross-correlation coefficient τ_p and the spacing between probes Δ_y, the average structure angle can be calculated [Eq. (1)]. The convection velocity U_c is about 690 m/s. The large-scale structure inclination angle varies from 36 to 56 deg to the flow direction depending on probe spacing. This variation suggests that the structure can no longer be assumed to be inclined at a constant angle.

Similar measurements were made at $x = 47$ cm (2240 θ_0); the results are shown in Fig. 9. In this case, channel 1 was held fixed at approximately the Mach 3 edge of the shear layer, whereas the upper probe (channel 2) was moved from station a to f into the Mach 5 freestream. In this case, the time delay τ_p is negative, which indicates that the "events" occur on the upper probe (channel 2) first and then on the fixed probe (channel 1) after a time delay. The large-scale structure angle again varies from about 36 to 56 deg (here $U_c \approx 710$ m/s). The result is essentially the same as that observed at the upstream station (in Fig. 8). The coherence functions for the same measurements are shown in Fig. 10. The two signals are highly coherent in the frequency range of 16–25 kHz, which corresponds to the dominant frequency of the large-scale structures. The coherence disappears as soon as the upper

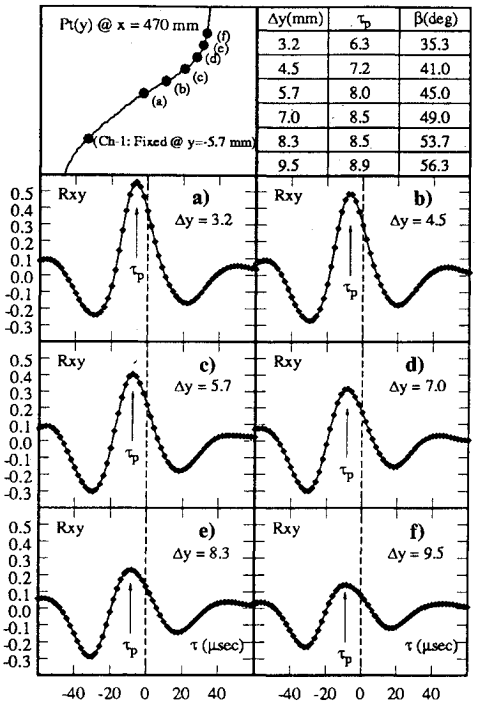

Fig. 9 Cross correlations at $x=47$ cm (variable probe spacing with fixed probe at $y=-5.7$ mm).

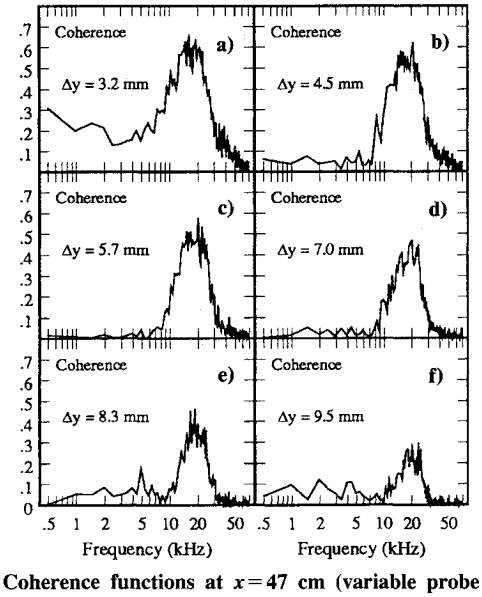

Fig. 10 Coherence functions at $x=47$ cm (variable probe spacing with fixed probe at $y=-5.7$ mm).

probe (channel 2) moves out of the shear layer into the Mach 5 freestream.

Two-point, fixed-spacing fluctuating pitot pressure measurements were also made at several streamwise stations to determine the variation in angle across the shear layer. The transducer's center-to-center spacing Δ_y is 4.16 mm. From the cross correlations, the average structure angles could again be determined. The results obtained at $x=22.9$ cm (1090 θ_0), 38.1 cm (1815 θ_0), and 48.3 cm (2300 θ_0) (the latter two stations are at essentially the same stations as for Figs. 8 and 9) are shown in Fig. 11a. Fixed-spacing dual normal hot-wire measurements were also made at $x=48.3$ cm (i.e., wire spacing Δ_y is about 2.54 mm). The results are also shown in Fig. 11a. At $x=22.9$ cm, the large-scale structures are inclined at a relatively constant angle of about 34–42 deg. At $x=38.1$ cm (i.e., downstream of the shock impingement), the large-scale structure angle is about 45 deg near the Mach 3 edge and increases to 58 deg near the Mach 5 edge. The measurements made at $x=48.3$ cm indicate that the structures are inclined at an angle of 40 deg near the Mach 3 edge, increasing to about 60 deg near the Mach 5 edge. The results obtained from the pitot pressure signals are slightly higher than those from hot-wire data. This may be due to the value of probe spacing Δ_y used, since the spatial resolution of the hot wire is much better than the Kulite pressure transducer. However, the difference in angle is small and within the uncertainty of the measurements.

The effects of shock impingement on the large-scale structures were also investigated from two-point fixed-spacing fluctuating pitot pressure measurements. Recall that the shear layer thickness δ_{rms} is nearly constant during the shock wave/shear layer interaction, then increases substantially, and finally returns to its undisturbed value. Since the rms thickness describes the vertical extent of the large-scale structure, the reaction of the large-scale structures to the shock impingement is essentially the same. The large-scale structure inclination angles β determined from cross correlations in the central part of the shear layer at several streamwise stations across the shock impingement are shown in Fig. 11b. The mean angle is about 38 deg in the region 17.8 cm$< x <$22.9 cm, increasing to about 43 deg just before the shock wave intercepts the shear layer (i.e., at $x\approx$25.4 cm). In the region of shock wave shear layer interaction (i.e., 27 cm$< x <$32 cm), the vertical extent of the large-scale structure remains the same, but the structure is stretched in the streamwise direction (the angle β decreases to about 33 deg). The angle β rapidly increases to about 50–55 deg just downstream of the shock impingement (i.e., 36 cm$< x <$38

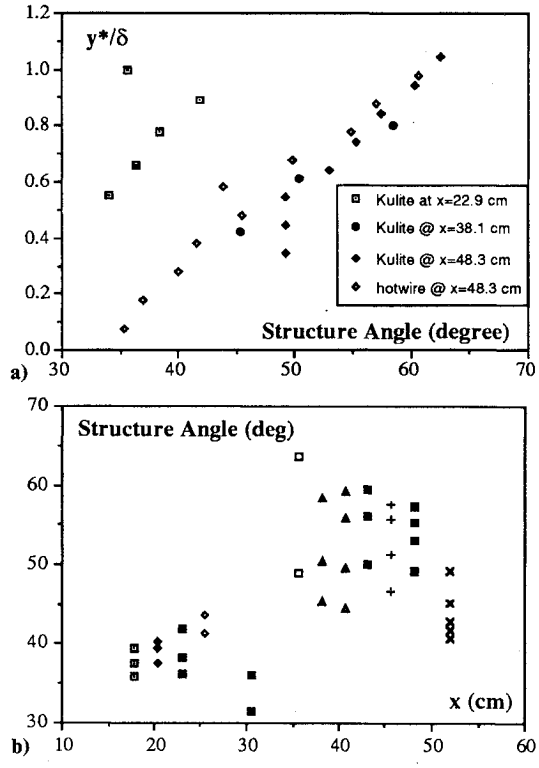

Fig. 11 a) Structure angle as a function of position in shear layer and b) structure angle as a function of streamwise position.

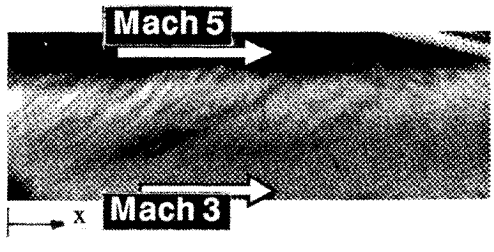

Fig. 12 Schlieren photograph spanning 18 cm$< x <$ 24 cm.

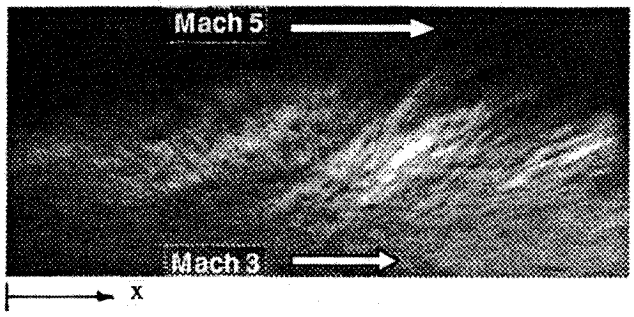

Fig. 13 Schlieren photograph spanning 43 cm < x< 51.6 cm.

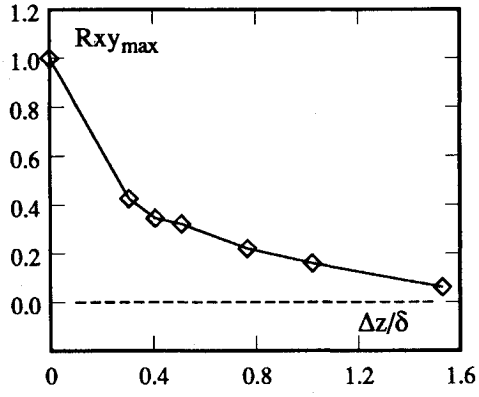

Fig. 14 Decay of maximum spanwise cross-correlation coefficients at x=47 cm.

cm) and retains this value for some distance (i.e., 38 cm< x<45 cm). Further downstream, the angle β gradually decreases to about 45 deg at about $x \approx 50$ cm. The stretching of the structure in the streamwise direction and the large increase in angle is believed to be responsible for the rapid growth of the shock impingement observed in the mean flow study.

Flow Visualization

A typical schlieren view of the shear layer between x=18 and 24 cm is shown in Fig. 12 (note that the flow direction is from left to right as indicated by the arrows). The mean shear layer development is relatively two-dimensional as expected, since the visual thickness agrees well with the pitot thickness and rms thickness along the centerline (i.e., z=0). A few recognizable large-scale structures are occasionally evident in the schlieren, as shown. As best as can be determined, the structures are inclined at about 33 deg, which agrees reasonably well with the results of fluctuating measurements (Fig. 11).

A schlieren photograph showing the shear layer between x=43 and 51.6 cm is shown in Fig. 13. Even though the power spectra show a strong peak, the lack of definition of the large-scale structures suggests that they are not quasi-two-dimensional as in incompressible cases.[5,23] Nevertheless, some indication of shape and size can be deduced from the photographs. Depending on the location and the photograph used, the structures appear to be inclined at angles from 42 to 48 deg, which agrees reasonably well with the flow measurements. In Fig. 13, the spacing between two large-scale structures is about 2.7 cm, which corresponds to a passage frequency of about 26 kHz. These results are also consistent with the power spectrum from fluctuating pitot pressure or mass-flux measurements.

Since the large-scale structures did not appear to be quasi-two-dimensional, the spanwise extent of the structures was further investigated using two-probe spanwise fluctuating pitot pressure measurements. From the decay of the maximum cross-correlation coefficient, Fig. 14, the spanwise extent of the large-scale structures is only about 1.0 to 1.5 shear layer thicknesses δ_{pt}. Browand and Ho[23] observed that the spanwise extent of the large-scale structures in an incompressible shear layer was about 4–5 shear layer vorticity thicknesses. By scaling distances from photographs, Clemens[6] showed that the spanwise extent of a supersonic shear layer with M_c=0.28 is about 1.9 shear layer visual thickness, which is somewhat higher than observed here.

Conclusions

An experimental study has been made to investigate the large-scale structures in a two-dimensional, high Reynolds number, turbulent free shear layer bounded by Mach 5 and 3 airstreams. Standard pitot pressure probe and pitot rake surveys were made to determine the shear layer growth rate, the two-dimensionality, and the mean flowfield in which it developed. Results show that the shear layer growth rate increases slightly due to impingement of a weak shock, but it returns to the undisturbed value within a short distance downstream. The shear layer growth rate based on pitot thickness agrees very well with those based on rms and visual thicknesses.

Two-point fluctuating pitot pressure measurements were made to investigate the large-scale structure at several stations from 127 to 520 mm (about 2450 initial momentum thicknesses θ_0) downstream of the shear layer origin. The power spectra are broadband but clearly show that the large-scale structures become progressively more organized with distance downstream, and at 2450 θ_0 downstream of the origin, their passage is responsible for a strong concentration of energy between 16 and 25 kHz. In nondimensional terms, the power spectra are centered at a Strouhal number of about 0.35. The large-scale structures are inclined at about 42–48 deg to the flow direction, which agrees very well with the results from schlieren photographs. Further, two-point spanwise fluctuating pitot pressure measurements show that the large-scale structures are three-dimensional even for the current case, which has a convective Mach number of about 0.28. The spanwise extent of the large-scale structure is only about 1.0–1.5 shear layer thicknesses. A preliminary study of the turbulent structures using fixed-spacing dual normal hot wires was also made at x=483 mm. Results obtained from the fluctuating pitot pressure measurements agree very well with the hot-wire results.

Acknowledgment

Support from the Office of Naval Research under Grant N0014-89-J-1221, monitored by P. Purtell and S. Lekoudis, is gratefully acknowledged.

References

[1]Lele, S. K., "Direct Numerical Simulation of Compressible Free Shear Flows," AIAA Paper 89-0374, AIAA 27th Aerospace Sciences Meeting, Reno, NV, Jan. 9–12, 1989.

[2]Bogdanoff, D. W., "Compressibility Effects in Turbulent Shear Layers," *AIAA Journal*, Vol. 21, No. 6, 1983, pp. 926, 927.

[3]Papamoschou, D., "Experimental Investigation of Heterogeneous Compressible Shear Layers," Ph.D Dissertation, California Inst. of Technology, Pasadena, CA, 1986.

[4]Ragab, S. A., and Wu, J. L., "Instabilities in the Free Shear Layer Formed by Two Supersonic Streams," AIAA Paper 88-0038, AIAA 26th Aerospace Sciences Meeting, Reno, NV, Jan. 8–12, 1988.

[5]Brown, G. L., and Roshko, A., "On Density Effects and Large Structures in Turbulent Mixing Layers," *Journal of Fluid Mechanics*, Vol. 64, Pt. 4, 1974, pp. 775–816.

[6]Clemens, N., "An Experimental Investigation of Scalar Mixing in Supersonic Turbulent Shear Layers," Stanford Univ., Stanford, CA, HTGL Rept. T-274, June 1991.

[7]Clemens, N. T., and Mungal, M. G., "Two- and Three-Dimensional Effects in the Supersonic Mixing Layer," AIAA Paper 90-1978, AIAA 28th Aerospace Sciences Meeting, Reno, NV, Jan. 8–11, 1990.

[8]Clemens, N. T., Mungal, M. G., Berger, T. E., and Vandsburger, U., "Visualizations of the Structure of the Turbulent Mixing Layer Under Compressible Conditions," AIAA Paper 90-0500, AIAA 28th Aerospace Sciences Meeting, Reno, NV, Jan. 8–11, 1990.

[9]Clemens, N. T., Paul, P. H., Mungal, M. G., and Hanson, R. K., "Scalar Mixing in the Supersonic Shear Layer," AIAA Paper 91-1720, AIAA 22nd Fluid Dynamics, Plasma Dynamics, and Lasers Conference, Honolulu, HI, June 24–26, 1991.

[10]Elliot, G. S., Samimy, M., and Reeder, M. F., "Pressure-Based, Real-Time Measurements in Compressible Free Shear Layers," AIAA Paper 90-

1980, AIAA/SAE/ASME/ASEE 26th Joint Propulsion Conference, Orlando, FL, July 1990.

[11]Elliott, G. S., and Samimy, M., "Compressibility Effects in Free Shear Layers," AIAA Paper 90-0705, AIAA 28th Aerospace Sciences Meeting, Reno, NV, Jan. 8–11, 1990.

[12]Messersmith, N. L., and Dutton, J. C., "An Experimental Investigation of Organized Structure and Mixing in Compressible Turbulent Free Shear Layers," Dept. of Mechanical and Industrial Engineering, Univ. of Illinois at Urbana-Champaign, UILU–ENG 92-4002, Urbana, IL, Jan. 1992.

[13]Sandham, N. D., and Reynolds,W. C., "Compressible Mixing Layer: Liner Theory and Direct Simulation," *AIAA Journal*, Vol. 28, No. 4, 1990, pp. 618–624.

[14]Shau, Y. R., and Dolling, D. S., "The Detection of Large Scale Structure in Undisturbed and Disturbed Compressible Turbulent Free Shear Layers," AIAA Paper 90-0711, AIAA 28th Aerospace Sciences Meeting, Reno, NV, Jan. 8–11, 1990.

[15]Shau, Y. R., "Experimental Study of Growth Rate Enhancement and Structure of Compressible Turbulent Free Shear Layers," Ph.D. Dissertation, Univ. of Texas at Austin, Austin, TX, 1990.

[16]Bendat, J. S., and Piersol, A. G., *Random Data: Analysis and Measurement Procedures*, 2nd ed., Wiley, New York, 1986.

[17]Papamoschou, D., "Structure of the Compressible Turbulent Shear Layer," AIAA Paper 89-0126, AIAA 27th Aerospace Sciences Meeting, Reno, NV, Jan. 1989.

[18]Fourguette, D., Dibble, R., and Mungal, M., "Time Evolution of the Shear Layer of a Supersonic Axisymmetric Jet at Matched Conditions," AIAA Paper 90-0508, AIAA 28th Aerospace Sciences Meeting, Reno, NV, Jan. 8–11, 1990.

[19]Hall, J. L., Dimotakis, P. E., and Rosemann, H., "Experiments in Non-Reacting Compressible Shear Layers," AIAA Paper 91-0629, AIAA 29th Aerospace Sciences Meeting, Reno, NV, Jan. 7–10, 1991.

[20]McIntyre, S., and Settles, G., "Optical Experiments on Axisymmetric Compressible Turbulent Mixing Layers," AIAA Paper 91-0623, AIAA 29th Aerospace Sciences Meeting, Reno, NV, Jan. 7–10, 1991.

[21]Dimotakis, P. E., "On the Convection Velocity of Turbulent Structures in Supersonic Shear Layers," AIAA Paper 91-1724, AIAA 22nd Fluid Dynamics, Plasma Dynamics, and Lasers Conference, Honolulu, HI, June 24–26, 1991.

[22]Shau, Y. R., and Dolling, D. S., "Exploratory Study of Turbulent Structure in Compressible Shear Layers Using Fluctuating Pitot Pressure Measurements," *Experiments in Fluids*, Vol. 12, 1992, pp. 293–306.

[23]Browand, F. K., and Ho, C. M., "The Mixing Layer: An Example of Quasi Two-Dimensional Turbulence," *Journal de Mécanique théorique et appliquée*, Numéro Spécial, 1983, pp. 99–120.